

ELECTRONIC SUPPORTING INFORMATION

Manganese and Iron PCP Pincer Complexes – The Influence of Sterics on Structure and Reactivity

Wolfgang Eder,^a Daniel Himmelbauer,^a Berthold Stöger,^b Luis F. Veiro,^d Marc Pignitter,^e and Karl Kirchner*,^a

^a Institute of Applied Synthetic Chemistry, Vienna University of Technology, Getreidemarkt 9, A-1060 Vienna, AUSTRIA

^b X-Ray Center, Vienna University of Technology, Getreidemarkt 9, A-1060 Vienna, AUSTRIA

^c Centro de Química Estrutural, Instituto Superior Técnico, Universidade de Lisboa, Av. Rovisco Pais No. 1, 1049-001 Lisboa, PORTUGAL

^d Department of Physiological Chemistry, Faculty of Chemistry, University of Vienna, Althanstrasse 14, 1090 Vienna, AUSTRIA

TABLE OF CONTENT

CRYSTALLOGRAPHIC DATA	S2-S3
EPR DATA	S3
NMR SPECTRA	S4-12

Crystallographic Data

Table S1. Details for the crystal structure determination of **2a, 3, 4**

	2a	3	4
formula	C ₂₃ H ₃₅ MnO ₃ P ₂	C ₂₃ H ₃₆ BF ₄ MnO ₃ P ₂	C ₂₂ H ₃₅ BrFeO ₂ P ₂
Fw, g mol ⁻¹	476.39	564.21	529.20
cryst.size, mm	0.25 x 0.25 x 0.2	0.15 x 0.15 x 0.04	0.52 x 0.24 x 0.10
color, shape	yellow, block	red, plate	yellow, block
crystal system	orthorhombic	monoclinic	orthorhombic
space group	Pbca (No. 61)	P2 ₁ (No. 4)	Pbca (No. 61)
a, Å	10.6082(2)	9.8863(9)	16.2190(15)
b, Å	15.4709(3)	11.4370(10)	13.5863(12)
c, Å	28.6193(5)	11.5482(10)	21.3867(19)
α, °	90	90	90
β, °	90	95.448(3)	90
γ, °	90	90	90
V, Å ³	4696.95(15)	1299.9(2)	4712.7(7)
T, K	100	100	100
Z, Z'	8, 1	2, 1	8, 1
ρ _{calc} , g cm ⁻³	1.347	1.442	1.492
μ, mm ⁻¹ (MoKα)	0.719	0.683	2.487
F(000)	2016	588	2192
absorption corrections, T _{min} -T _{max}	multi-scan, 0.62 - 0.74	multi scan, 0.68 - 0.75	multi scan, 0.18 - 0.27
θ range, deg	34.92 - 2.39	33.16 - 2.51	32.602 - 2.175
no. of rflns measd	37035	34239	58434
R _{int}	0.00382	0.0636	0.0700
no. of rflns unique	10249	9908	8605
no. of rflns I>2σ(I)	8469	7963	6117
no.of params/restraints	270 / 0	329 / 1	261/0
R (I > 2σ(I)) ^a	0.0696	0.0411	0.0318
R (all data)	0.0414	0.0611	0.0638
wR (I > 2σ(I))	0.0301	0.0747	0.0672
wR (all data)	0.0746	0.0816	0.0787
GooF	1.003	0.977	1.019
Diff.Four.peaks min/max, eÅ ⁻³	-0.500 / 0.609	-0.622 / 0.457	-0.493 / 0.645
CCDC no.	2097016	2097017	2097018

Table S2. Details for the crystal structure determination of **5b** and **5c**

	5b	5c
formula	C ₂₄ H ₃₉ FeO ₄ P ₂	C ₂₂ H ₃₅ FeO ₂ P ₂
Fw, g mol ⁻¹	509.34	449.29
cryst.size, mm	0.35 x 0.25 x 0.16	0.27 x 0.20 x 0.02
color, shape	green, brick	green, plate
crystal system	triclinic	orthorhombic
space group	P-1 (No. 2)	Pbca (No. 61)
a, Å	13.4933(18)	15.387(13)
b, Å	25.671(3)	14.266(11)
c, Å	38.134(5)	20.780(19)
α, °	86.404(5)	90
β, °	87.601(4)	90
γ, °	79.813(4)	90
V, Å ³	12969(3)	4562(7)
T, K	100	100
Z, Z'	20, 10	8, 1
ρ _{calc} , g cm ⁻³	1.304	1.308
μ, mm ⁻¹ (MoKα)	0.731	0.815
F(000)	5420	1912
absorption corrections, T _{min} -T _{max}	multi-scan, 0.49 - 0.42	multi-scan, 0.74 - 0.40
θ range, deg	30.17 - 1.07	22.54 - 2.18
no. of rflns measd	332470	5687
R _{int}	0.1159	0.0666
no. of rflns unique	75997	2968
no. of rflns I > 2σ(I)	27731	2287
no. of params/restraints	2931 / 0	252 / 0
R (I > 2σ(I)) ^a	0.0593	0.0703
R (all data)	0.1698	0.0983
wR (I > 2σ(I))	0.1446	0.1635
wR (all data)	0.1994	0.1784
GooF	0.996	1.133
Diff.Four.peaks min/max, eÅ ⁻³	-0.629 / 1.421	-0.498 / 1.241
CCDC no.	2097019	2097020

EPR Data

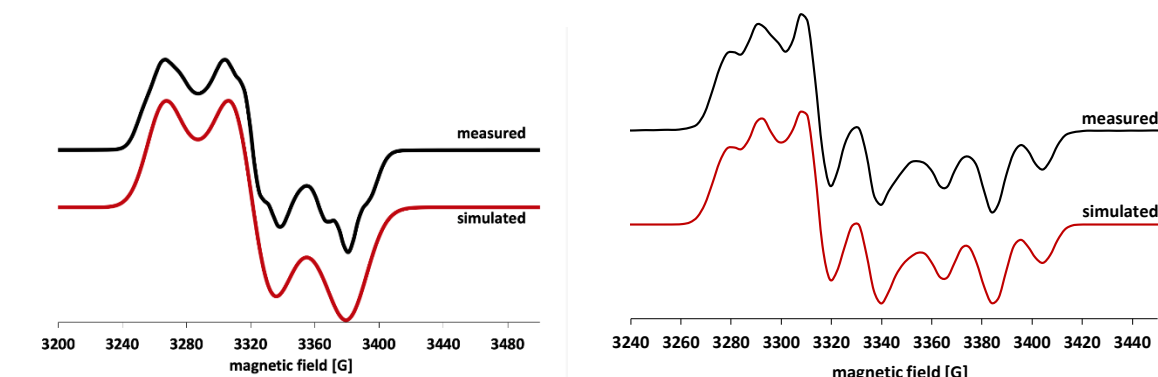


Figure S1. X-band EPR spectra of [Fe(κ^3P, C, P -PCP^{CH₂-tBu})(CO)₂] (**5b**) (left) and [Fe(κ^3P, C, P -PCP^{O-tBu})(CO)₂] (**5c**) (right) in toluene glass at 100 K at a microwave frequency of 9.86 GHz. The red line represents a simulation with $g_x = 2.051$, $g_y = 2.027$, $g_z = 2.010$, $A_x = 45.0$ G, $A_y = 39.3$ G, and $A_z = 48.5$ G (**5b**) and $g_x = 2.044$, $g_y = 2.034$, $g_z = 1.991$, $A_x = 20.3$ G, $A_y = 22.5$ G, and $A_z = 14.5$ G (**5c**).

NMR spectra

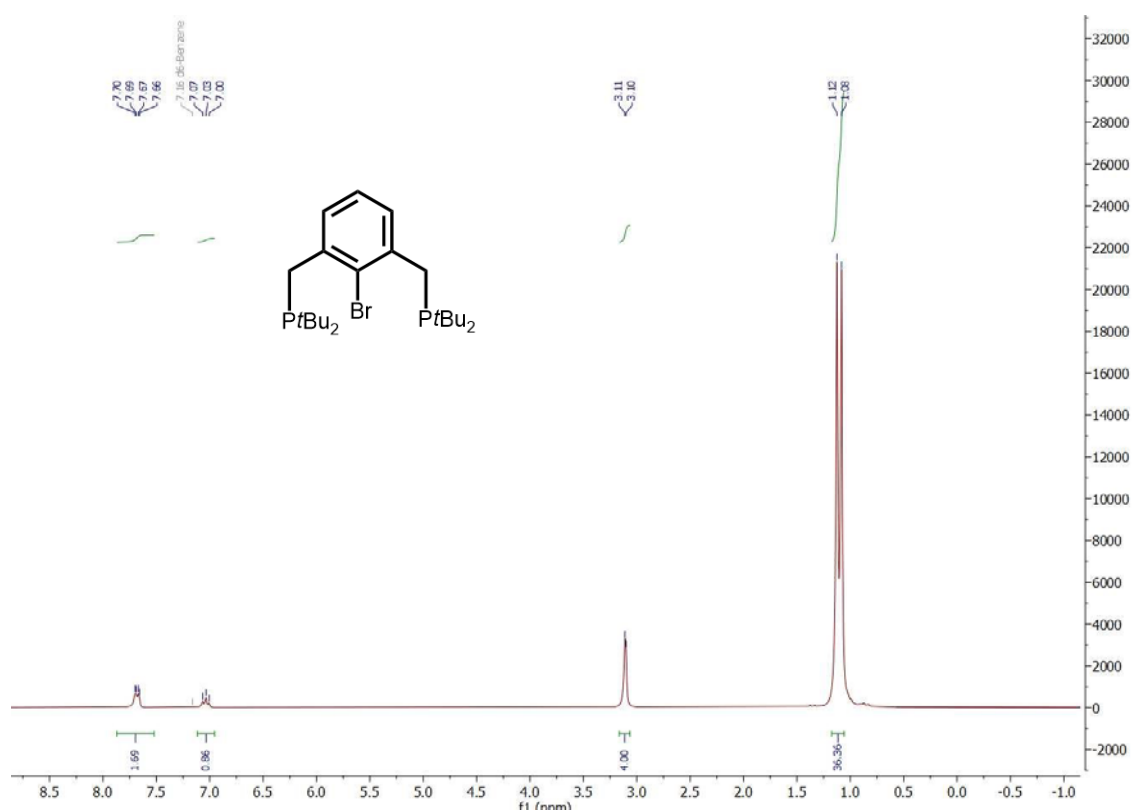


Figure S2. ¹H-NMR spectrum of **1a** (250 MHz, C₆D₆)

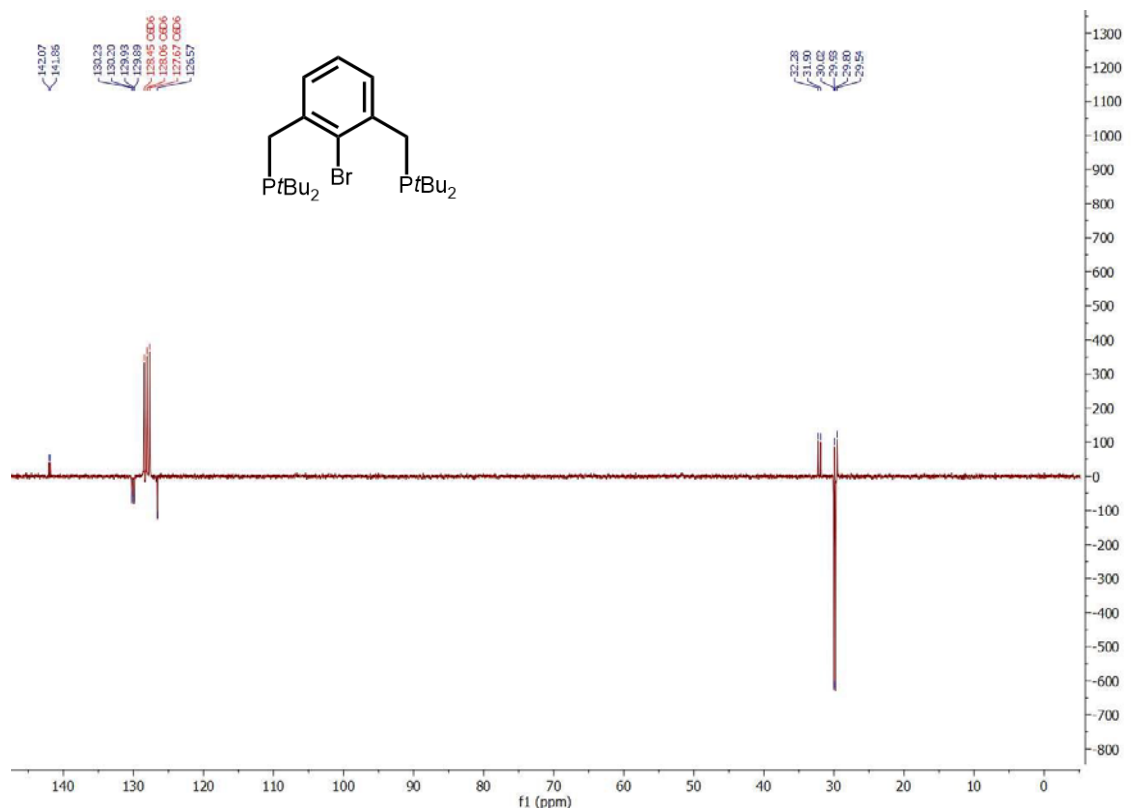


Figure S3. ¹³C{¹H} APT NMR spectrum of **1d** (63 MHz, C₆D₆)

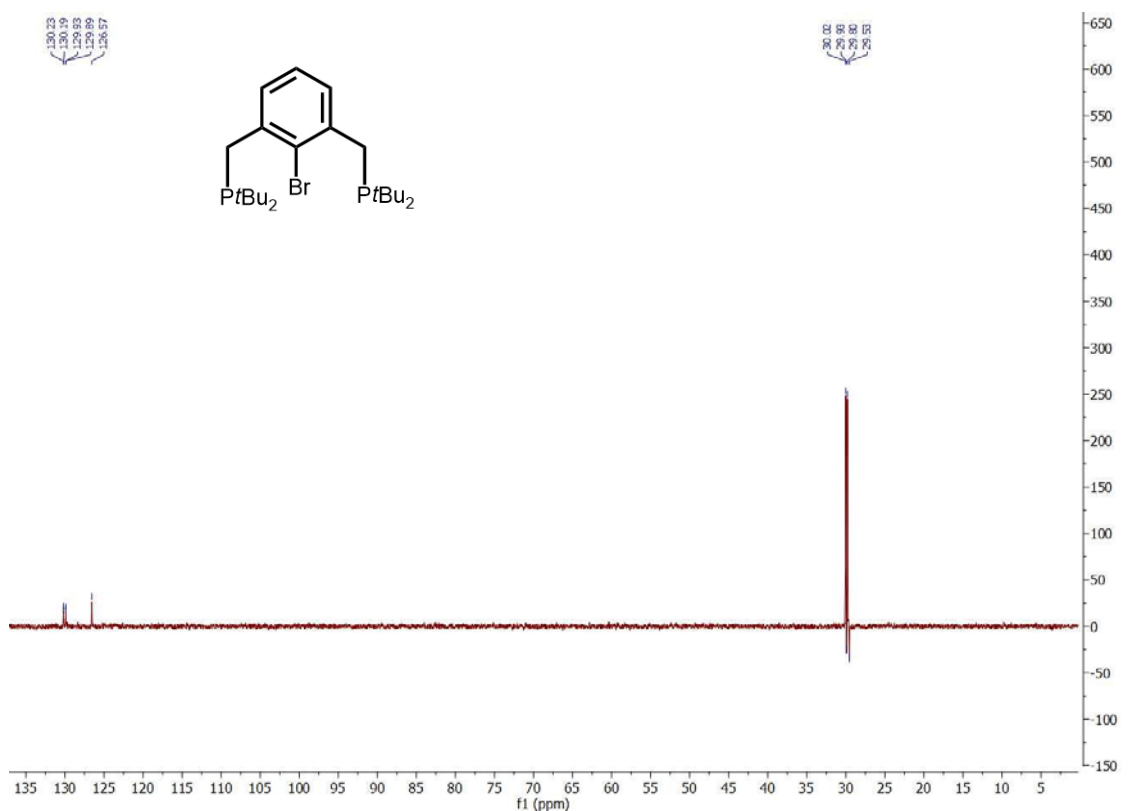


Figure S4. $^{13}\text{C}\{\text{H}\}$ DEPT NMR spectrum of **1d** (63 MHz, C_6D_6)

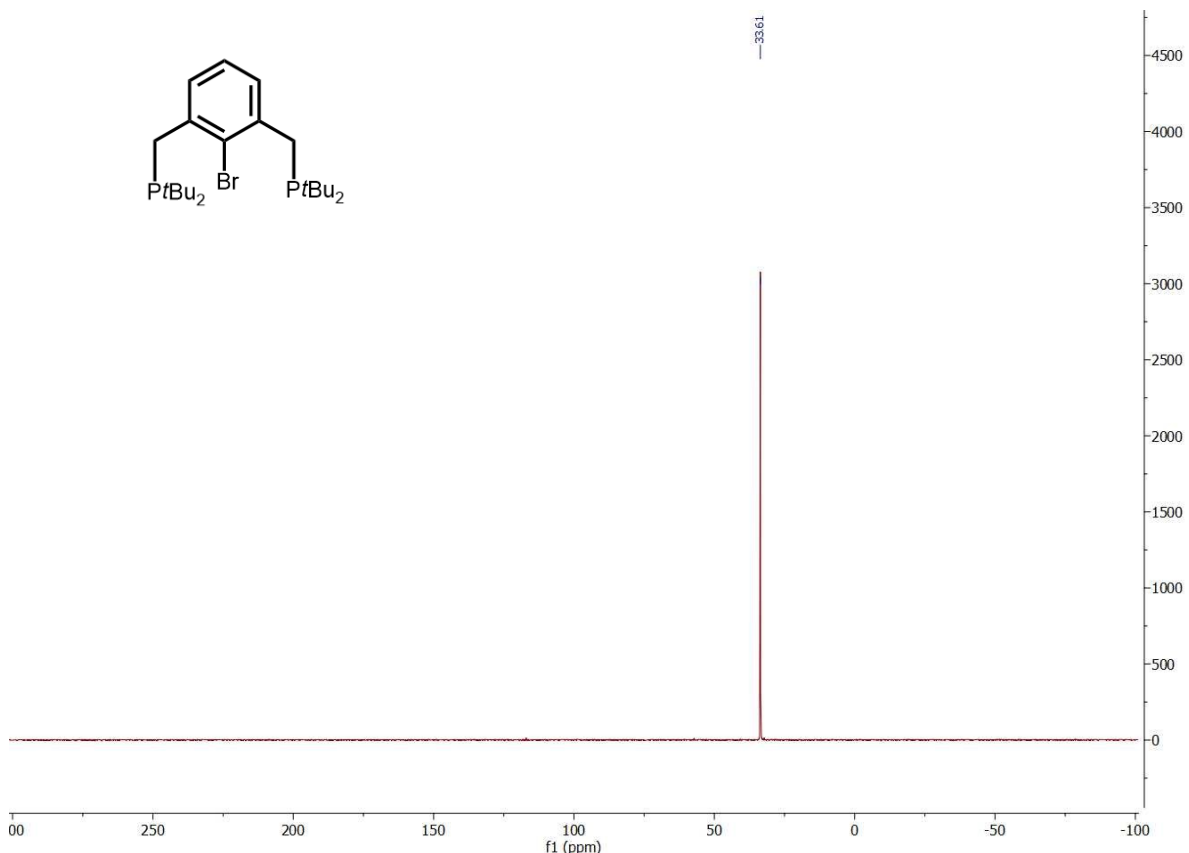


Figure S5. $^{31}\text{P}\{\text{H}\}$ NMR spectrum of **1d** (101 MHz, C_6D_6)

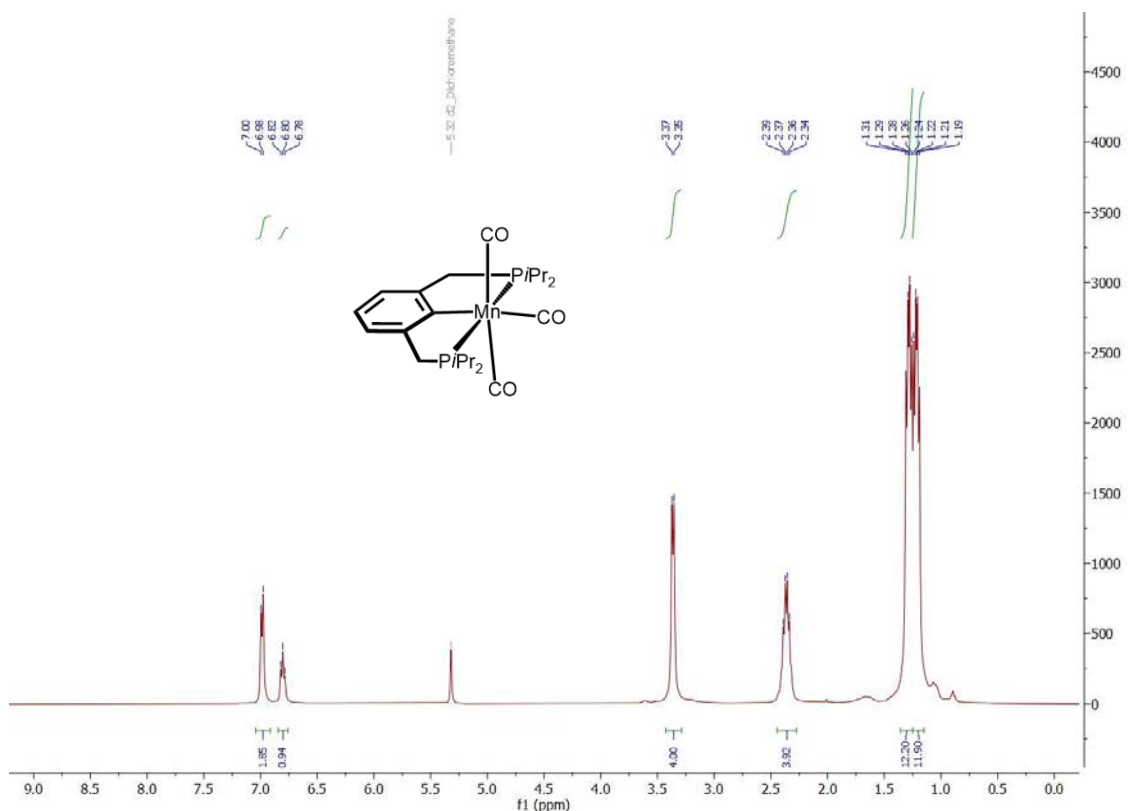


Figure S6. ^1H NMR spectrum of **2a** (400 MHz, CD_2Cl_2)

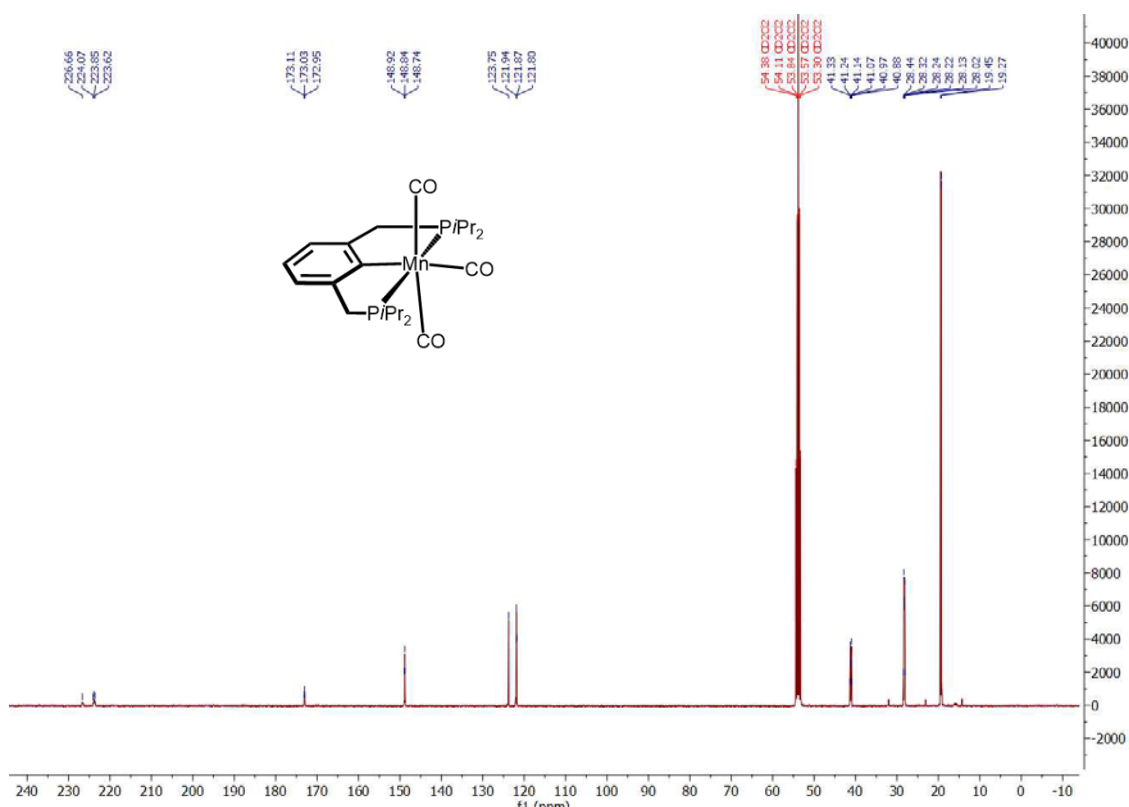


Figure S7. $^{13}\text{C}\{^1\text{H}\}$ NMR spectrum of **2a** (101 MHz, CD_2Cl_2)

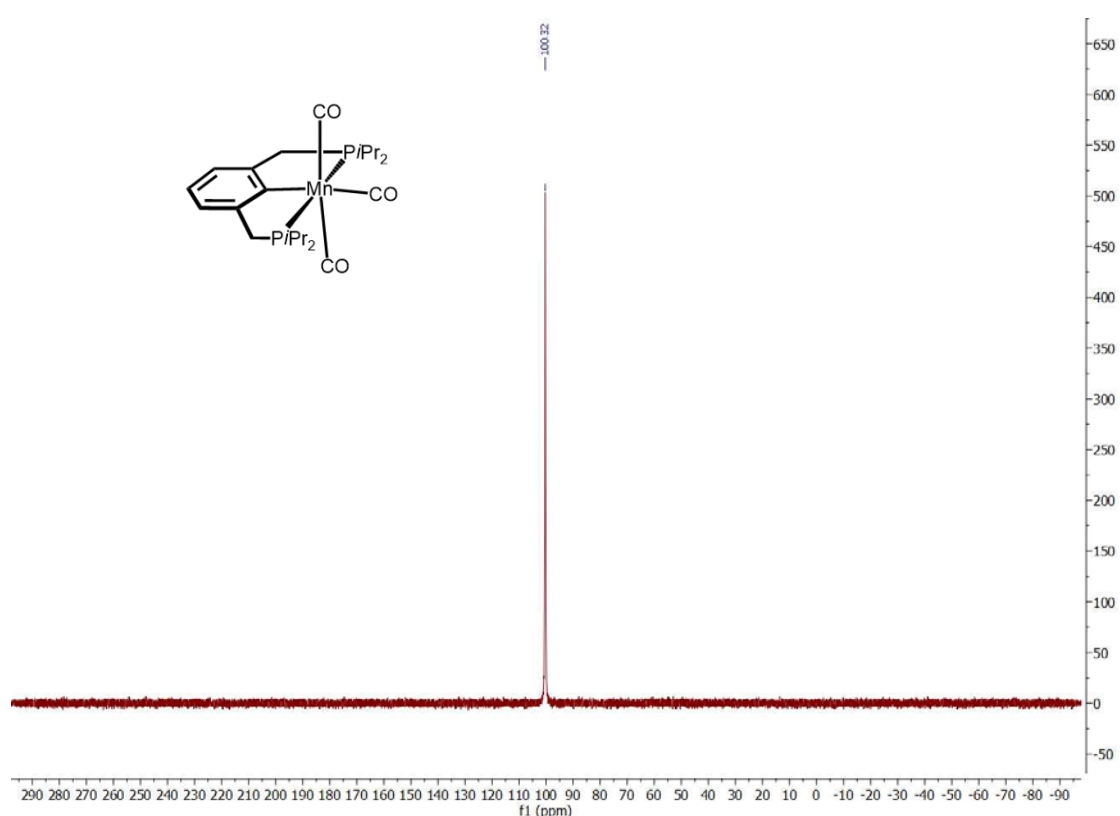


Figure S8. $^{31}P\{^1H\}$ NMR spectrum of **2a** (162 MHz, CD_2Cl_2)

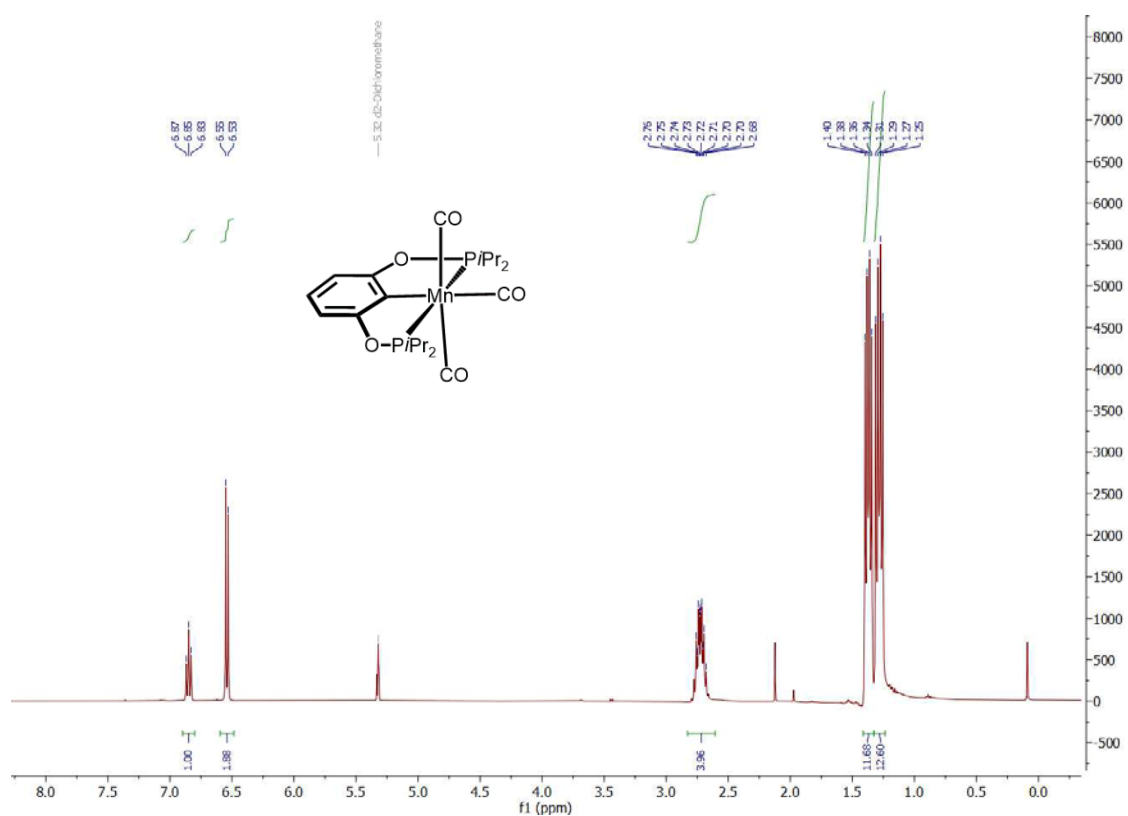


Figure S9. 1H NMR spectrum of **2b** (400 MHz, CD_2Cl_2)

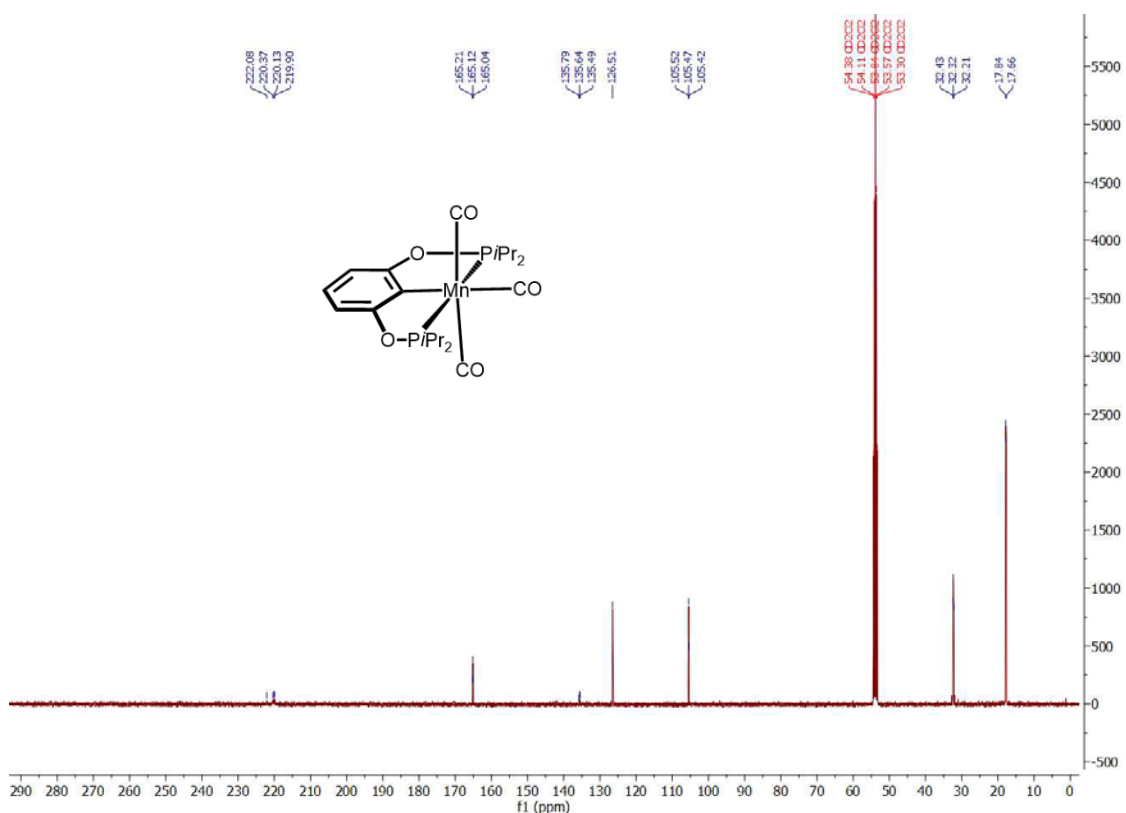


Figure S10 $^{13}\text{C}\{\text{H}\}$ NMR spectrum of **2b** (101 MHz, CD_2Cl_2)

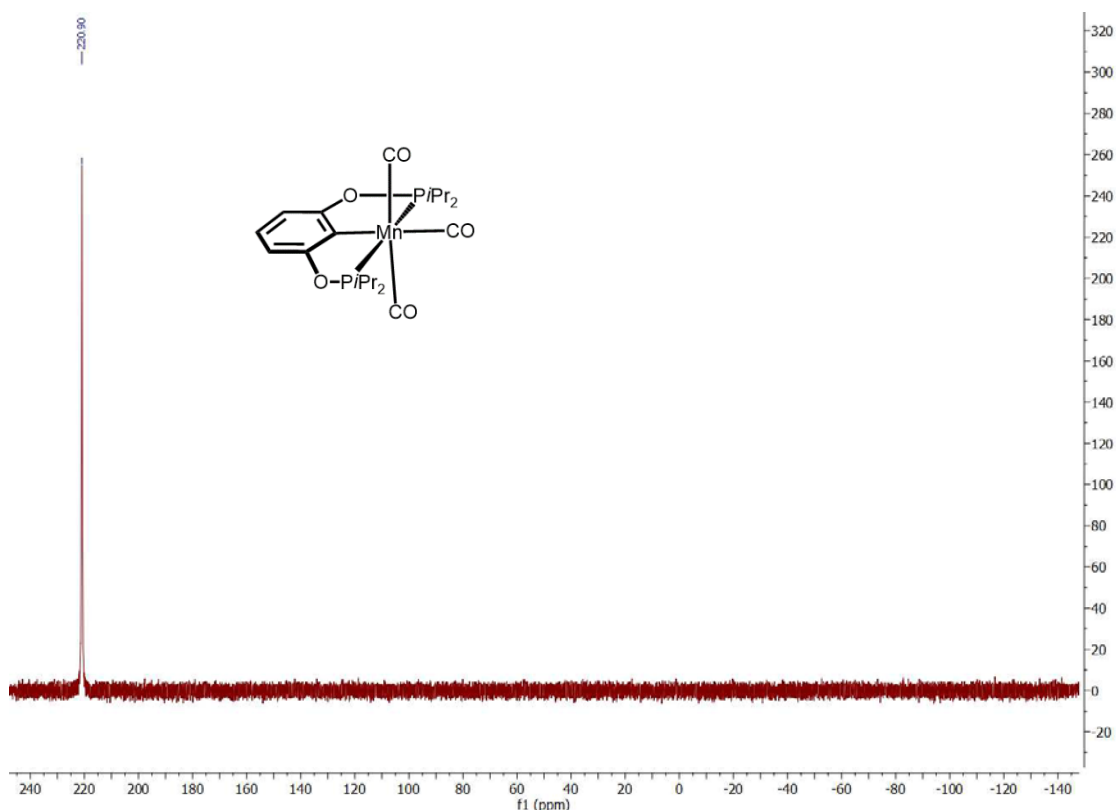


Figure S11. $^{31}\text{P}\{\text{H}\}$ NMR spectrum of **2b** (162 MHz, CD_2Cl_2)

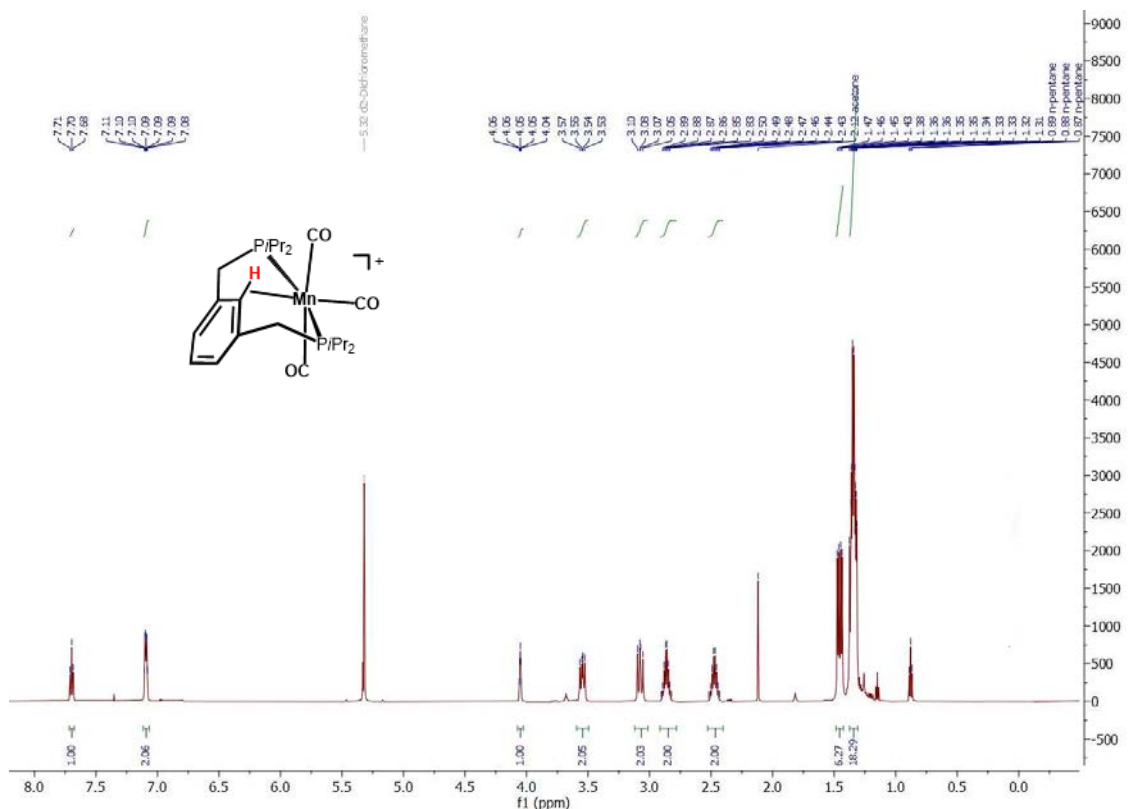


Figure S12. ^1H NMR spectrum of **3** (600 MHz, CD_2Cl_2)

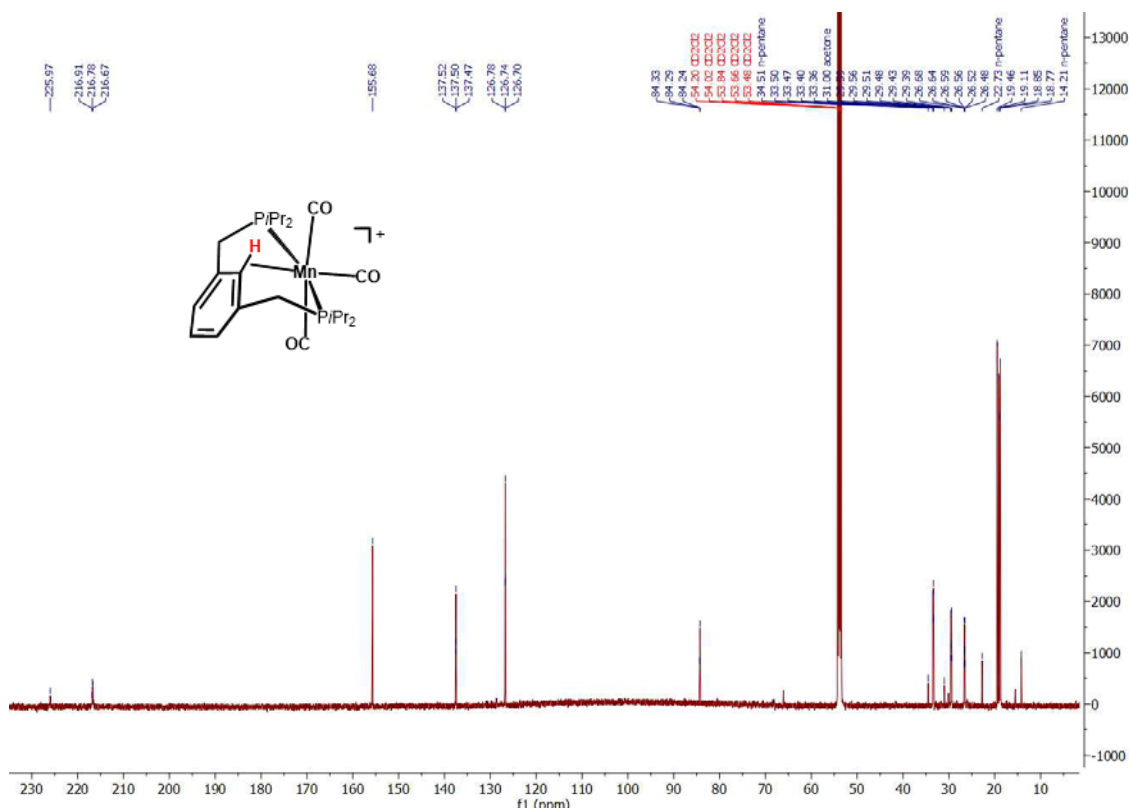


Figure S13. $^{13}\text{C}\{\text{H}\}$ NMR spectrum of **3** (151 MHz, CD_2Cl_2)

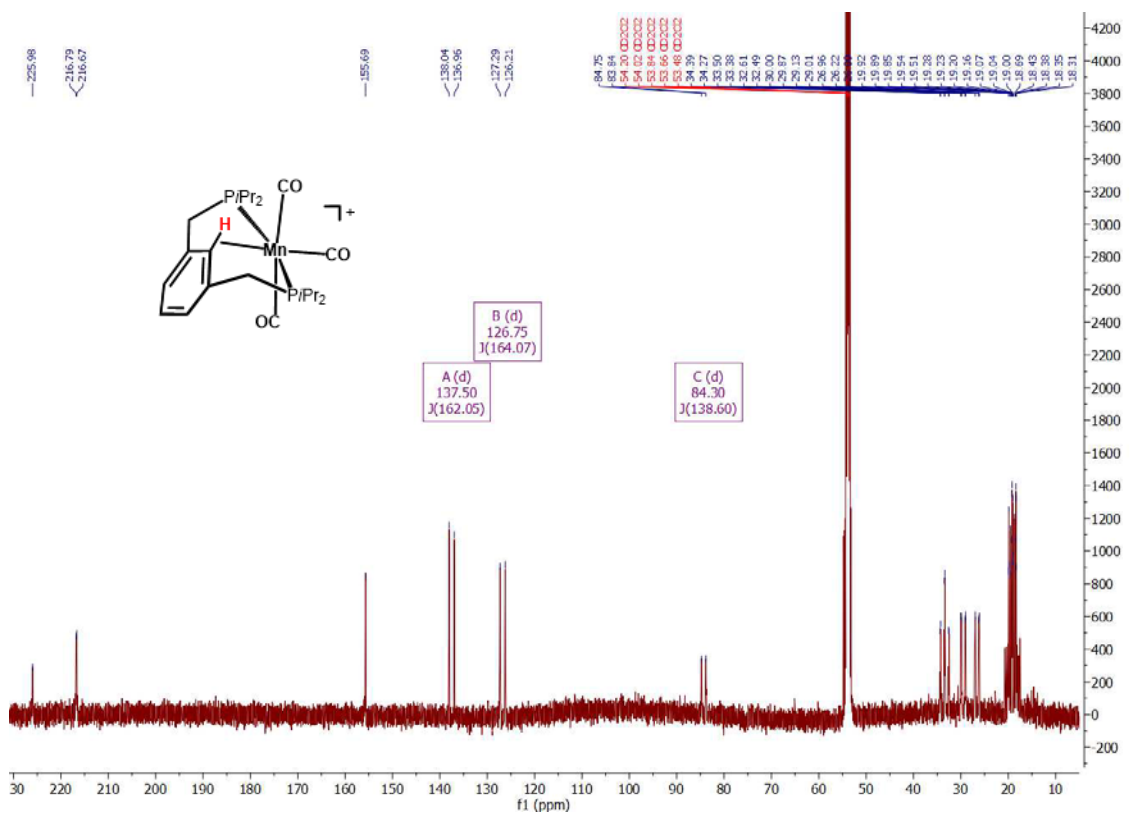


Figure S14. ^{13}C NMR spectrum of **3** (151 MHz, CD_2Cl_2)

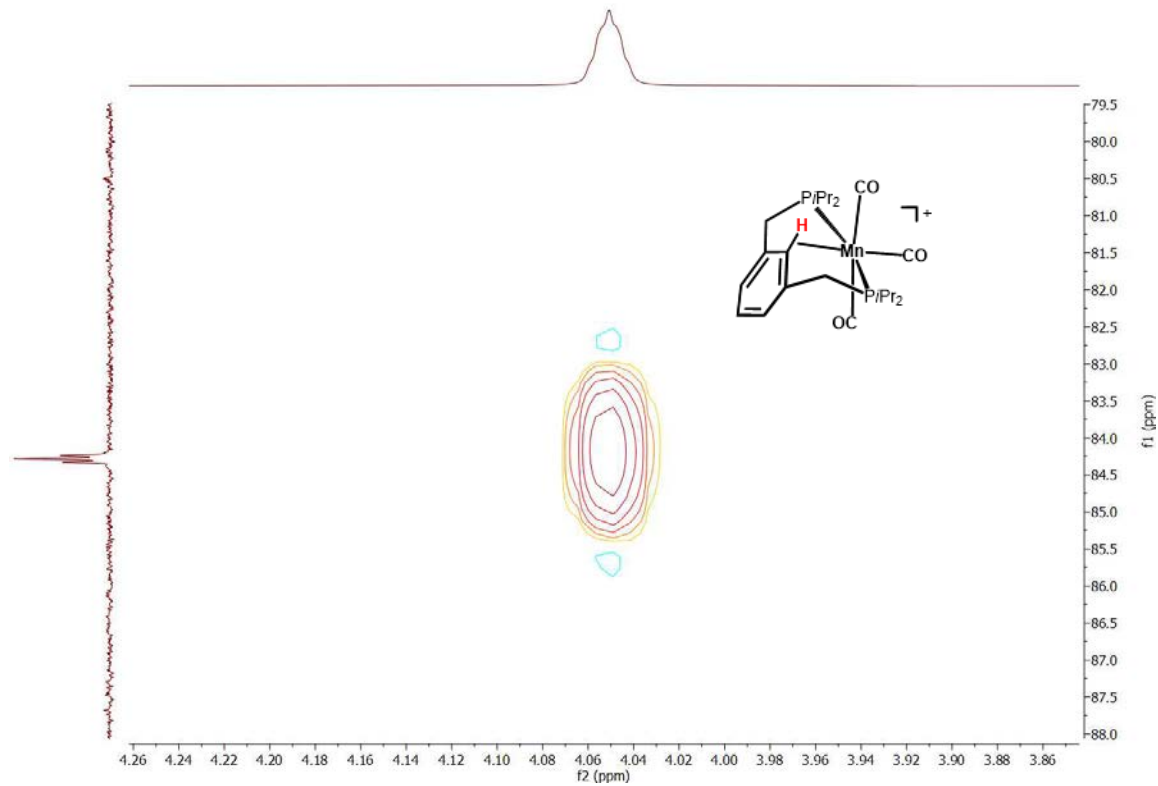


Figure S15. section of the HSQC NMR spectrum of **3** depicting the cross-peak of the agostic C-H bond

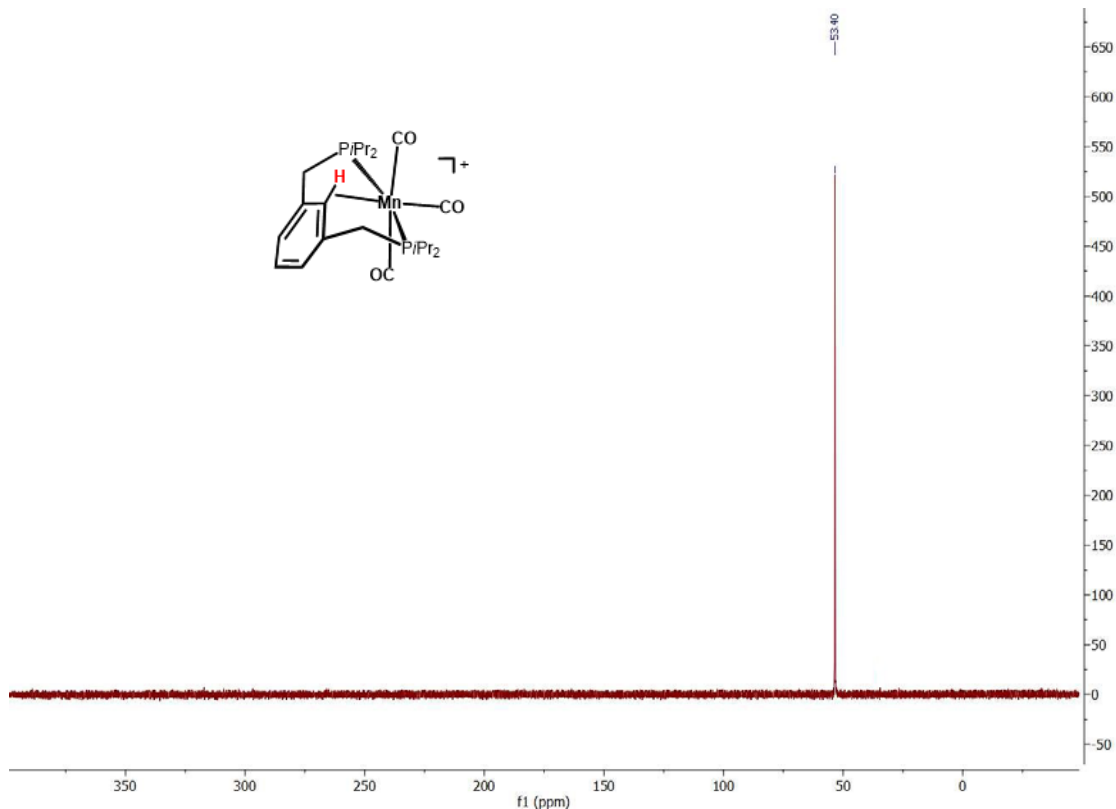


Figure S16. $^{31}P\{^1H\}$ NMR spectrum of **3** (243 MHz, CD_2Cl_2)

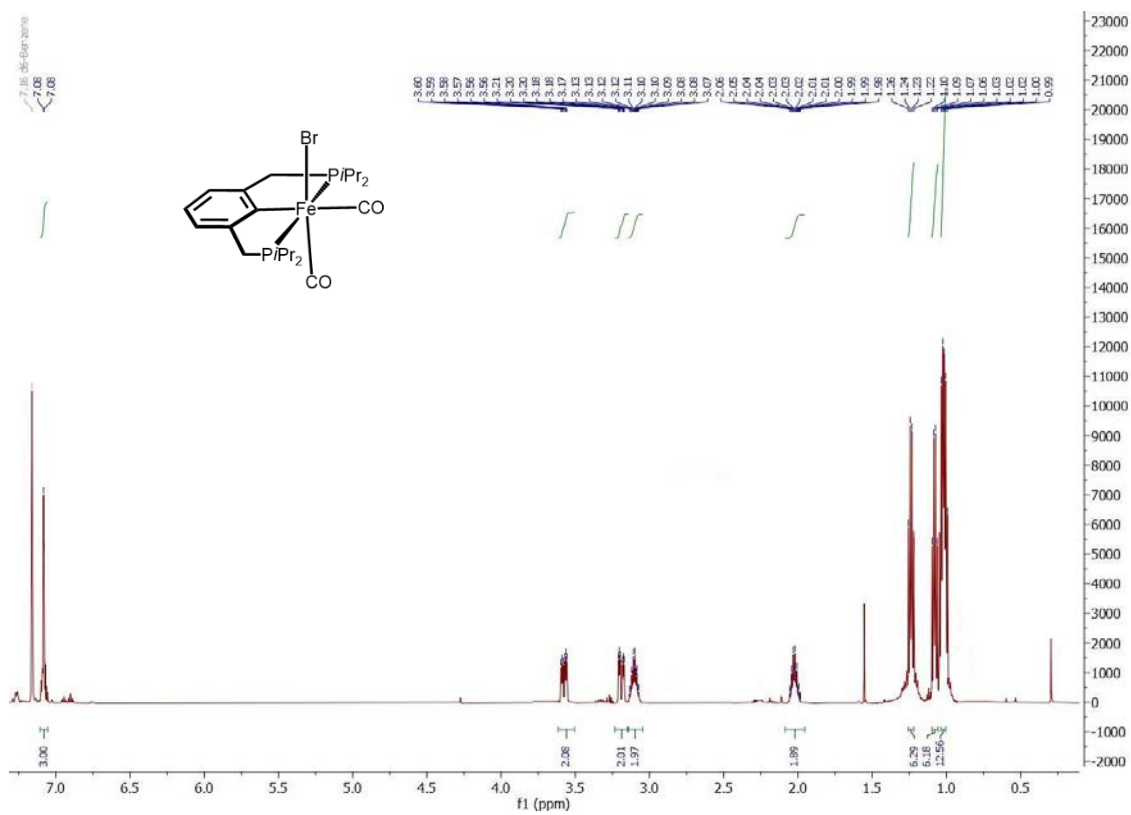


Figure S17. 1H NMR spectrum of **4** (600 MHz, C_6D_6)

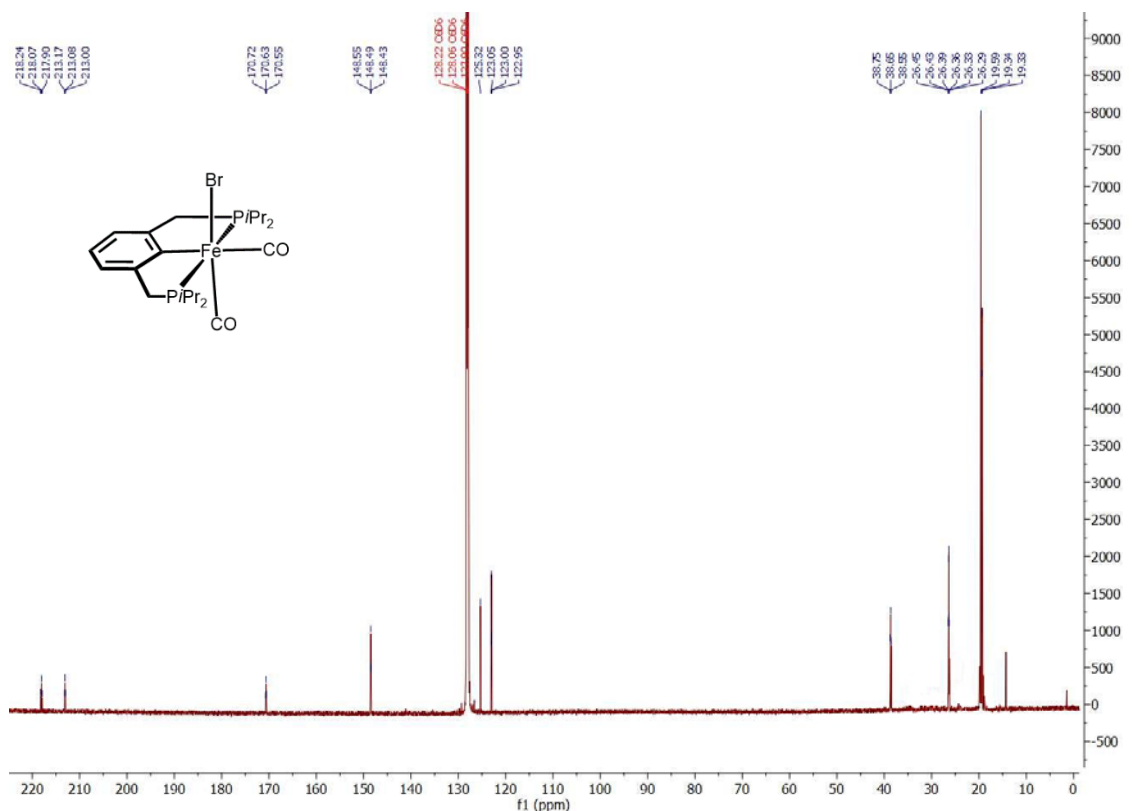


Figure S18. $^{13}\text{C}\{^1\text{H}\}$ NMR spectrum of **4** (151 MHz, C_6D_6)

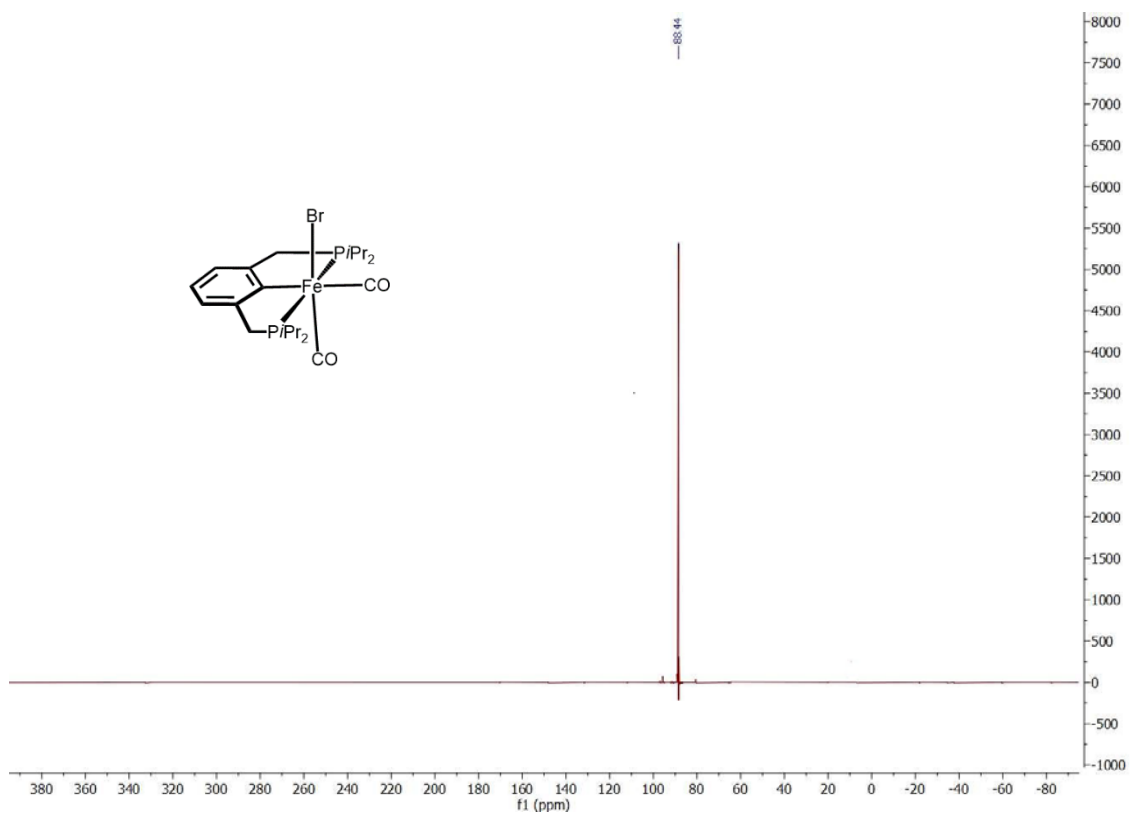


Figure S19. $^{31}\text{P}\{^1\text{H}\}$ NMR spectrum of **4** (243 MHz, C_6D_6)